2-25-2009

A Double Layer Surface Traction Free Green's Tensor

Darko Volkov
Worcester Polytechnic Institute, darko@wpi.edu

SIAM J. APPL. MATH.
Vol. 69, No. 5, pp. 1438–1456

A DOUBLE LAYER SURFACE TRACTION FREE GREEN'S TENSOR*

DARKO VOLKOV†

Abstract. A double layer Green's tensor for linear elasticity in half space is computed. Traction free conditions on the surface are imposed making this Green's tensor relevant in geophysics for modeling displacements caused by slips on faults. Past attempts at computing related Green's tensors are discussed. Applications to computing displacement fields by integration over fault regions or by use of asymptotic estimates are presented.

Key words. linear elasticity, Green's tensors in half space, traction free surface, cracks in half space, slip along cracks

AMS subject classifications. 74B05, 86-08, 86A17

DOI. 10.1137/080723697

1. Introduction.

Inside a linear elastic region Ω with Lamé coefficients $\lambda > 0$ and $\mu > 0$, a displacement field u satisfies the equation

$$\mu\Delta u + (\lambda+\mu)\nabla \mathrm{div}\, u = 0 \text{ in } \Omega \tag{1}$$

or alternatively

$$\mathrm{div}\,\sigma = 0 \text{ in } \Omega, \tag{2}$$

where the stress tensor is given by

$$\sigma_{ij}(u) = \lambda\, \mathrm{div}\, u\, \delta_{ij} + \mu(\partial_i u_j + \partial_j u_i).$$

We will use the following notation for stress vectors in the normal direction n throughout this paper:

$$T_n u = \sigma(u)n.$$

The natural basis for $\mathbb{R}^3$ will be denoted by (e_1, e_2, e_3). If Ω is unbounded, a finite energy condition for displacements is required:

$$\int_\Omega \sigma(u) : \epsilon(u) < \infty, \tag{3}$$

where we have used the strain tensor $\epsilon_{ij}(u) = \frac{1}{2}(\partial_i u_j + \partial_j u_i)$ and the dot product between two 3×3 matrices A and B defined by $A : B = \mathrm{tr}(A^T B)$. If Ω is the whole space $\mathbb{R}^3$, it is known since Kelvin that the tensor

$$G_{ij}(x,y) = \frac{1}{8\pi\mu(\lambda+2\mu)}((\lambda+\mu)\partial_{x_i} r\partial_{x_j} r + (\lambda+3\mu)\delta_{ij})\frac{1}{r}, \tag{4}$$

*Received by the editors May 8, 2008; accepted for publication (in revised form) October 14, 2008; published electronically February 25, 2009. This work was partially supported by NSF grant DMS 0707421.
http://www.siam.org/journals/siap/69-5/72369.html
†Department of Mathematical Sciences, Worcester Polytechnic Institute, Worcester, MA 01609 (darko@wpi.edu).

where $r = \sqrt{(x_1 - y_1)^2 + (x_2 - y_2)^2 + (x_3 - y_3)^2}$, satisfies Green's problem

$$\mu \Delta G + (\lambda + \mu) \nabla \operatorname{div} G = -I_3 \delta_y \text{ in } \mathbb{R}^3, \tag{5}$$

where I_3 is the 3×3 identity matrix. In addition G decays at infinity and has finite energy away from the singularity at $x = y$,

$$\int_{\mathbb{R}^3 \setminus B(y,1)} \sigma(G(x,y)) : \epsilon(G(x,y)) dx < \infty. \tag{6}$$

Let Γ be a bounded fault or cut in the space $\mathbb{R}^3$. It is possible to use tensor G to find an integral representation for displacement fields in $\mathbb{R}^3$ that are continuous across Γ and whose stress vector has a given discontinuity (sometimes called jump) across Γ; see [5].

We are interested in this paper in elastic displacement fields in the half space $x_3 < 0$, denoted by $\mathbb{R}^{3-}$, that are traction free on the surface $x_3 = 0$, satisfy some discontinuity condition across a bounded surface Γ in $\mathbb{R}^{3-}$, and decay at infinity while having finite energy. Such displacement fields u can be expressed as integrals on Γ involving Green's tensor M which satisfies

$$\mu \Delta M + (\lambda + \mu) \nabla \operatorname{div} M = -I_3 \delta_y \text{ in } \mathbb{R}^{3-}, \tag{7}$$

$$T_{e_3} M = 0 \text{ on the surface } x_3 = 0, \tag{8}$$

$$M \text{ decays at infinity and } \int_{\mathbb{R}^{3-} \setminus B(y,1)} \sigma(M(x,y)) : \epsilon(M(x,y)) dx < \infty. \tag{9}$$

Mindlin was the first to compute a tensor of this type; see [4]. Sheu performed an analogous computation in the anisotropic case; see [7]. In that same paper he was able to reconstruct displacement fields produced by the 1999 Jiji, Taiwan earthquake using his new Green's tensor.

If u is a finite energy elastic displacement field in the half space $\mathbb{R}^{3-}$ that has zero traction on the surface $x_3 = 0$ and satisfies some discontinuity condition across a bounded surface Γ in $\mathbb{R}^{3-}$, then u can be expressed as the integral over Γ of M against some density which solves an adequate boundary integral equation. These equations on Γ were studied by Martin, Päivärinta, and Rempel in [3].

It might be costly and nontrivial to solve the boundary integral equations discussed in [3]. However, this can be avoided altogether in some cases. Assume that we want to solve for a (finite energy, decaying at infinity) displacement field u such that

$$\mu \Delta u + (\lambda + \mu) \nabla \operatorname{div} u = 0 \text{ in } \mathbb{R}^{3-} \setminus \Gamma, \tag{10}$$

$$T_{e_3} u = 0 \text{ on the surface } x_3 = 0, \tag{11}$$

$$u \text{ is continuous across } \Gamma, \tag{12}$$

$$[T_n u] = f \text{ is a given jump across } \Gamma; \tag{13}$$

then u is given by the integral formula

$$u = \frac{1}{2} \int_\Gamma M f. \tag{14}$$

Note that the free space analogue of problem (10), (12), and (13) is given by the field $u = \frac{1}{2} \int_\Gamma G f$ (see [5]), and from there integral formula (14) is easily conceived in half

space. Let us now examine the adjoint problem to (10)–(13), namely, solving for a (finite energy, decaying at infinity) displacement field u such that

$$\mu\Delta u + (\lambda+\mu)\nabla \mathrm{div}\, u = 0 \text{ in } \mathbb{R}^{3-} \setminus \Gamma, \tag{15}$$

$$T_{e_3} u = 0 \text{ on the surface } x_3 = 0, \tag{16}$$

$$T_n u \text{ is continuous across } \Gamma, \tag{17}$$

$$[u] = g \text{ is a given jump across } \Gamma. \tag{18}$$

We know from [5] that the free space analogue of this problem has the solution $u = \frac{1}{2}\int_\Gamma (T_{n(y)}G)^T g$, where, as previously, G is Kelvin's Green's tensor and $T_{n(y)}$ is the stress vector in the y dependent normal direction $n(y)$. The main result of this paper is to find Green's tensor H such that problem (15)–(18) has the solution $u = \frac{1}{2}\int_\Gamma Hg$ for any smooth tangential vector field on Γ, g. Note that some authors have incorrectly thought that H could be simply given by $(T_{n(y)}M)^T$; this is not true for the operators $T_{e_3(x)}$ and $(T_{n(y)}\cdot)^T$ do not commute when applied to Mindlin's Green's tensor M. We verified this using a symbolic computer software. Actually, this lack of a commutativity property can be understood on simple examples. We discuss three such simple examples in this paper. Steketee was the first author to offer a correct approach on how to compute Green's tensor H; see [6]. Interestingly, he was able to give a full solution only in Fourier space, and he was able to complete his computation in section 7 of his paper [6] in only one particular case.

We now outline the contents of this paper. In section 2 we present our method for computing Green's tensor H. We do not provide any explicit calculations. They are a good order of magnitude more complex than those of Mindlin's because we have to start from the derivative of Kelvin's tensor. It was actually possible for us to perform this calculation thanks to the use of a symbolic calculus software. We indicate the form of the final solution in the appendix. In effect, we are able to provide relatively concise formulas for H only on the surface $x_3 = 0$. For $x_3 < 0$, the simplest form for H is too lengthy to appear in this paper. Note, however, that this formula for H is still malleable using a symbolic calculus software, and it can then be turned into any computer language code. We also demonstrate in section 2 how our Green's tensor relates to two-dimensional (2D) linear elasticity in a half plane. Assuming that displacements occur only in one direction, we are able to recover Green's scalar function in the lower half plane with zero Neumann condition on the surface. In section 3 we explain why under some decay and growth condition, at infinity and near singular points, our Green's tensor is unique, and we use this uniqueness result to verify our (long!) calculation for H. We also include in section 3 a paragraph aimed at understanding why past attempts at computing Green's tensor H were erroneous and why discrepancies were not picked up on numerical data. In section 4 we use our tensor H for the explicit numerical computation of surface displacement fields due to a slip on a crack, or fault, beneath the surface. We note that the exact solution given by $u = \frac{1}{2}\int_\Gamma Hg$ might require a costly computation, which is undesirable in applications where such a direct computation would have to be iterated a large number of times. We found a way to obtain an approximate field $u(x_1, x_2, 0)$ based on asymptotics that just assume that (x_1, x_2) is some distance away from the fault Γ. We also evaluate in section 4 the error incurred in making that approximation. We then discuss in that same section an interesting symmetry property, valid for deep faults.

2. Assembling Green's tensor H. We start from the well-known Kelvin Green's tensor G given by (4). Let $n(y)$ be a y dependent normal direction. We

define a double layer potential by setting

$$\tilde{G}(x,y,n) = (T_{n(y)}G(x,y))^T. \tag{19}$$

2.1. The image method. The image method consists of combining $\tilde{G}(x,y,n)$ with terms from

$$(T_{\overline{n}(y)}G(x,\overline{y}))^T,$$

where $\overline{n} = (n_1, n_2, -n_3)$ and $\overline{y} = (y_1, y_2, -y_3)$, in such a way to obtain vanishing traction on the plane $x_3 = 0$, along the x_1 and x_2 directions. More precisely, set

$$\tilde{\tilde{G}}_{ij}(x,y) = \tilde{G}_{ij}(x,y,n) + \tilde{G}_{ij}(x,\overline{y},\overline{n}) \text{ for } 1 \le i \le 3, \quad 1 \le j \le 2,$$
$$\tilde{\tilde{G}}_{i3}(x,y) = \tilde{G}_{i3}(x,y,n) - \tilde{G}_{i3}(x,\overline{y},\overline{n}) \text{ for } 1 \le i \le 3.$$

If g is a smooth vector field on Γ, then $u(x) = \frac{1}{2}\int_\Gamma \tilde{\tilde{G}}(x,y)g(y)$ satisfies (15), (17), and (18), has finite elastic energy, and decays at infinity. However, (16) is only partially satisfied; only the first two components of $T_{e_3}u$ are zero at $x_3 = 0$. Consequently, to find Green's function H, we need to solve three Boussinesq problems with data

$$-F_j := T_{e_3(x)}\tilde{\tilde{G}}_{3j}(x,y)|_{x_3=0}, \quad j = 1,2,3, \tag{20}$$

to compensate for the nonzero $T_{e_3}u \cdot e_3$ term on the surface $x_3 = 0$.

2.2. A Fourier method for solving Boussinesq problems. We find it most efficient to follow the method outlined by Steketee [6]. Recall the definition of Boussinesq half space elasticity problems: find v of finite elastic energy in $\mathbb{R}^{3-}$ such that

$$\mu\Delta v + (\lambda+\mu)\nabla \mathrm{div}\, v = 0 \text{ in } \mathbb{R}^{3-}, \tag{21}$$
$$T_{e_3}u \cdot e_i = 0 \text{ on the surface } x_3 = 0, \quad i = 1,2, \tag{22}$$
$$T_{e_3}u \cdot e_3 = -F \text{ on the surface } x_3 = 0. \tag{23}$$

The solution to (21)–(23) can be sought in terms of a Galerkin vector $(0,0,\gamma)$, where γ is biharmonic in the lower plane $x_3 < 0$. Indeed, if a displacement field v is in the form

$$v = \left(-\alpha\partial_1\partial_3\gamma,\, -\alpha\partial_2\partial_3\gamma,\, \left[(1-\alpha)\partial_3\partial_3 + \partial_1^2 + \partial_2^2\right]\gamma\right), \text{ where } \alpha = \frac{\lambda+\mu}{\lambda+2\mu}, \tag{24}$$

then it satisfies (21). Note that $\frac{1}{2} < \alpha < 1$. The stress vector $T_{e_3}v$ simplifies as

$$\sigma_{13}(v) = \mu\partial_1(\Delta - 2\alpha\partial_3\partial_3)\gamma,$$
$$\sigma_{23}(v) = \mu\partial_2(\Delta - 2\alpha\partial_3\partial_3)\gamma,$$
$$\sigma_{33}(v) = \partial_3((\lambda(1-\alpha)+2\mu)\Delta - 2\alpha\mu\partial_3\partial_3)\gamma.$$

Starting from the problem

$$\Delta^2\gamma = 0 \text{ in } x_3 < 0, \tag{25}$$
$$\sigma_{13}(v) = \sigma_{23}(v) = 0 \text{ on } x_3 = 0, \tag{26}$$
$$\sigma_{33}(v) = -F \text{ on } x_3 = 0, \tag{27}$$
$$\gamma \text{ is bounded as } x_3 \to -\infty, \tag{28}$$

we perform a Fourier transform of γ in the first two variables only. A long calculation leads to

$$\hat{\gamma}(\xi, x_3) = \left(-\frac{1}{2} \frac{(-1+2\,\alpha)}{|\xi|^3 \alpha\, \pi^3} + \frac{x_3}{\pi^2 |\xi|^2} \right) \hat{F} \frac{1}{8\,(\mu+\lambda)\,(\alpha-1)} e^{2\,\pi\,|\xi| x_3}, \tag{29}$$

where Fourier transforms are given by

$$\hat{F}(\xi_1, \xi_2) = \iint e^{2\pi i (x_1 \xi_1 + x_2 \xi_2)} F(x_1, x_2) dx_1 dx_2.$$

$\hat{v}$ can be now found according to formula (24). Finally, applying an inverse Fourier transform to $\hat{v}$ will give a finite energy, decaying at infinity, vector field v which satisfies the elasticity equations in $\mathbb{R}^{3-}$ and whose stress vector at the surface $x_3 = 0$ satisfies (26) and (27).

2.3. The Boussinesq solution in our case. Can the vector field v defined in the previous paragraph be given in a closed form? The answer is yes if F is the force coming from adding to Kelvin's tensor its image above the plane $x_3 = 0$ and computing, for each column, the resulting vertical traction at $x_3 = 0$; this will yield Mindlin's tensor. In our case the forcing term F is given by (20); this case involves more terms, of higher degree, compared to those appearing in the derivation of Mindlin's solution. Steketee was able to carry out such a computation in section 7 of his paper [6] in only one particular case. At the time of his work, symbolic algebra software was not available, and this greatly limited investigators' ability to manipulate large expressions. Going back to our work, let us give, for illustration, the expression of F_1, the forcing term for the first Boussinesq problem that we need to solve. F_1 is the ratio of

$$\begin{aligned} \big((2\,\mu+\lambda)\,\mu^2 {x_1}^4 + \big((\mu+2\,\lambda)\,\mu^2 {x_2}^2 - {y_3}^2\,(13\,\lambda+11\,\mu)\,\mu^2 \big)\,{x_1}^2 + (\lambda-\mu)\,\mu^2 {x_2}^4 \\ + {y_3}^2\,(\mu+2\,\lambda)\,\mu^2 {x_2}^2 + {y_3}^4\,(2\,\mu+\lambda)\,\mu^2 \big) n_1 \\ + \big(3\,\mu^3 x_2 {x_1}^3 + \big(3\,\mu^3 {x_2}^3 - 3\,{y_3}^2\,(4\,\mu+5\,\lambda)\,\mu^2 x_2 \big)\,x_1 \big)\, n_2 \\ + \big(-3\,y_3\,(\mu+\lambda)\,\mu^2 {x_1}^3 + \big(-3\,y_3\,(\mu+\lambda)\,\mu^2 {x_2}^2 + 12\,{y_3}^3\,(\mu+\lambda)\,\mu^2 \big)\,x_1 \big)\, n_3 \end{aligned}$$

to

$$\left({x_1}^2 + {x_2}^2 + {y_3}^2 \right)^{7/2} \pi\,\mu\,(2\,\mu+\lambda)\,.$$

To compute v given by (24)–(29), for $F = F_j$, $j = 1, 2, 3$, we first computed the Fourier transform $\hat{F}$, which we multiplied by adequate terms to find $\hat{\gamma}$ according to formula (29). We then proceeded to compute the inverse Fourier transform of $\hat{\gamma}$, from which the expression for v, solution to (21)–(23), follows from (24). Corresponding double integrals were evaluated in polar coordinates. A symbolic calculation software had to be used due to the length and complexity of the expressions involved. Of particular importance for polar angle integration was the use of the following integrals:

$$\int_0^{2\pi} e^{iz\cos\theta} \cos p\theta d\theta = (i)^p 2\pi J_p(z), \tag{30}$$

where p is an integer and J_p is the Bessel function of the first kind of order p. This formula can be derived from formula (9.1.21) in [1]. As to integration in radius, a formula for

$$\int_0^\infty \frac{J_q(2\pi\rho r)\rho^p}{(\rho^2 + y_3^2)^{\frac{7}{2}}} d\rho, \quad p = 1, \ldots, 5, \quad q = 0, \ldots, 4 \quad y_3 < 0, \quad r > 0, \tag{31}$$

was needed. For compuation of inverse Fourier transforms the following was also needed

$$\int_0^\infty e^{2\pi r x_3} J_p(2\pi\rho r) r^q dr \quad p = 0, \ldots, 4 \quad q = 0, \ldots, 2, \quad x_3 < 0, \quad \rho > 0, \tag{32}$$

Closed forms for (31), (32), albeit intricate, can be computed. The final expression for H is intricate and involves many terms. We discuss it in the appendix.

2.4. Symmetry properties. We first notice that Green's tensor H depends on x_1, y_1, x_2, and y_2 only through $x_1 - y_1$ and $x_2 - y_2$.

2.4.1. Switching the first two coordinates. Let (t_1, t_2, t_3) be a vector in $\mathbb{R}^3$. Denote by $u = (u_1, u_2, u_3)$ the vector $H(t_1, t_2, t_3)$. (u_1, u_2, u_3) is a function of $x_1 - y_1$, $x_2 - y_2$, $x_3 \leq 0$, $y_3 \leq 0$, (n_1, n_2, n_3), (t_1, t_2, t_3), $\lambda > 0$, and $\mu > 0$. The following relations hold:

$$u_1(x_1 - y_1, x_2 - y_2, n_1, n_2, t_1, t_2) = u_2(x_2 - y_2, x_1 - y_1, n_2, n_1, t_2, t_1), \tag{33}$$

$$u_3(x_1 - y_1, x_2 - y_2, n_1, n_2, t_1, t_2) = u_3(x_2 - y_2, x_1 - y_1, n_2, n_1, t_2, t_1). \tag{34}$$

Physically, they express that the first and the second coordinate play the same role for the displacement vector Ht.

2.4.2. Switching the normal vector n and the source vector t. Computations indicate that the coordinates of Ht depend on the normal vector n and on t only through

$$n_1 t_1, \quad n_2 t_2, \quad n_3 t_3, \quad n_1 t_2 + n_2 t_1, \quad n_1 t_3 + n_3 t_1, \quad n_2 t_3 + n_3 t_2,$$

and, consequently,

$$u(n, t) = u(-n, -t), \tag{35}$$

and

$$u(n, t) = u\left(\frac{t}{|t|}, n|t|\right). \tag{36}$$

Symmetry property (35) corresponds to reversing the orientation on the fault Γ. Symmetry property (36) expresses that the displacements caused by a concentrated slip of vector t, on an infinitesimal fault of normal vector n, are the same as the displacements caused by a concentrated slip of vector $n|t|$, on an infinitesimal fault of normal vector $t/|t|$. We will give in a subsequent section another interpretation of this symmetry property valid for deeper faults of finite size.

2.5. Relation to 2D elasticity. Two dimensional scalar elasticity is the limit model of general elasticity as boundary conditions are constant along a given direction, say, x_2, and displacements take place only in the x_2 direction. We assume here that the fault Γ introduced earlier is linear and infinite in the x_2 direction; thus, a normal vector to Γ satisfies $n_2 = 0$. We then integrate the vector He_2 in x_2 in the range $(-\infty, \infty)$. A long computation leads, after simplification, to the vector

$$\left(0, \frac{(x_1 - y_1)\left({x_3}^2 + {y_3}^2 + (x_1 - y_1)^2\right) n_1 + y_3\left({x_3}^2 - {y_3}^2 - (x_1 - y_1)^2\right) n_3}{\pi\left((x_1 - y_1)^2 + (x_3 - y_3)^2\right)\left((x_1 - y_1)^2 + (x_3 + y_3)^2\right)}, 0\right). \tag{37}$$

Next, we show that this is in agreement with the 2D model. It is known that

$$g(x_1,y_1,x_3,y_3) = -\frac{1}{4}\frac{\ln\left((x_1-y_1)^2+(x_3-y_3)^2\right)}{\pi} - \frac{1}{4}\frac{\ln\left((x_1-y_1)^2+(x_3+y_3)^2\right)}{\pi}$$

is the half plane $x_3 < 0$ Green's function for the 2D Laplacian in the x_1, x_3 coordinates that satisfies the zero Neumann condition $\partial_{x_3} g = 0$ at $x_3 = 0$. Note that $\partial_{x_3}\partial_{y_1} g$ and $\partial_{x_3}\partial_{y_3} g$ are also zero at $x_3 = 0$. Computing

$$\partial_{y_1} g\, n_1 + \partial_{y_3} g\, n_3,$$

we find exactly the second coordinate of the vector given in (37).

Remark. The scalar operators $\partial_{x_3}, \partial_{y_1}$, and ∂_{y_3} do commute. However, we wish to emphasize that, in 3D elasticity, the argument cannot be as simple since the traction operators $T_{e_3(x)}$ and $(T_{e_j(y)}\cdot)^T$ are not commutative.

3. Verification. We were able to devise a way of verifying our long computation resulting in a closed form for the tensor H.

3.1. A uniqueness theorem.

THEOREM 3.1. *There is a unique tensor $A(x,y)$, for x and y in $\mathbb{R}^{3-}$, whose entries are measurable functions in (x,y) and which satisfies the following equations:*

$$\mu\Delta_x A(x,y) + (\lambda+\mu)\nabla_x \mathrm{div}_x A(x,y) = 0 \text{ in } \mathbb{R}^{3-} \text{ if } x \neq y, \tag{38}$$

$$T_{e_3(x)} A(x,y) = 0 \text{ on the surface } x_3 = 0 \text{ if } y_3 < 0, \tag{39}$$

$$|A(x,y)| \leq \frac{C}{|x|} \text{ as } y \text{ is fixed and } |x| \to \infty, \tag{40}$$

$$|\nabla_x A(x,y)| \leq \frac{C}{|x|^2} \text{ as } y \text{ is fixed and } |x| \to \infty, \tag{41}$$

$$|A(x,y) - \tilde{G}(x,y,n)| \leq C \text{ as } y \text{ is fixed and } x \to y, \tag{42}$$

$$|\nabla_x (A(x,y) - \tilde{G}(x,y,n))| \leq C \text{ as } y \text{ is fixed and } x \to y, \tag{43}$$

where C is a constant independent of x and $\tilde{G}$ is defined by (19).

Proof. It is clear that our Green's tensor $H(x,y)$ satisfies conditions (38)–(43). To show uniqueness, assume that A_1 and A_2 satisfy (38)–(43) and set $\overline{A} = A_1 - A_2$. Then as $\overline{A}(x,y)$ and $\nabla_x \overline{A}(x,y)$ are bounded for x and y, $x \neq y$, in $\mathbb{R}^{3-}$, $\overline{A}$ satisfies the elasticity equations everywhere in $\mathbb{R}^{3-}$. Next, if $\overline{A}_j$ is the jth column of $\overline{A}$, let B_R be the subset of $\mathbb{R}^3$ defined by $\{x : |x| \leq R \text{ and } x_3 \leq 0\}$. Applying conditions (38)–(41) and integrating by parts,

$$\int_{B_R} \varepsilon\left(\overline{A}_j\right) : \sigma\left(\overline{A}_j\right) = \int_{\partial B_R} T_n\left(\overline{A}_j\right)\overline{A}_j.$$

Applying boundary condition (39) and decay at infinity (40)–(41), we find that

$$\int_{\mathbb{R}^{3-}} \varepsilon\left(\overline{A}_j\right) : \sigma\left(\overline{A}_j\right) = 0.$$

$\overline{A}_j$ is then a rigid displacement which, due to the imposed decay at infinity, must be zero. ∎

3.2. Application to verifying our calculation for the tensor H. Equations (38) and (39) were verified directly. Conditions (40) and (41) are satisfied with an additional order of magnitude for H, that is,

$$|H(x,y)| \le \frac{C}{|x|^2} \text{ as } y \text{ is fixed and } |x| \to \infty,$$
$$|\nabla_x H(x,y)| \le \frac{C}{|x|^3} \text{ as } y \text{ is fixed and } |x| \to \infty.$$

More precisely, each entry of $H(x,y)$ is asymptotically equivalent as $|x| \to \infty$, to the ratio of some homogeneous polynomial of degree 11 in $x_1, x_2, x_3, \sqrt{x_1^2+x_2^2}$, and $\sqrt{x_1^2+x_2^2+x_3^2}$ to $(x_1^2+x_2^2)^3(x_1^2+x_2^2+x_3^2)^{\frac{7}{2}}$.

H also satisfies conditions (42) and (43); they express that $H(x,y)$ and $\tilde{G}(x,y,n)$ have the same type of singularity as y approaches x.

3.3. The problem with past attempts at finding Green's tensor H. Some authors have incorrectly thought that H could be simply given by $(T_{n(y)}M)^T$; this is not true for the operators $T_{e_3(x)}$ and $(T_{n(y)}\cdot)^T$ do not commute when applied to Mindlin's Green's tensor M. We verified this fact using a symbolic computer software; note, however, that this lack of a commutativity property can be understood on simple examples. We discuss such simple examples below.

Example 1. For the vector $v(x,y) = (0,0,x_1y_3)$, $T_{e_3(x)}v = (\mu y_3, 0, 0)$. Let A be the 3×3 matrix (v,v,v); that is, each column of A is v. The first column of $(T_{e_3(y)}T_{e_3(x)}A)^T$ is computed to be equal to (μ^2, μ^2, μ^2), while the first column of $T_{e_3(x)}(T_{e_3(y)}A)^T$ is $(0,0,0)$.

Example 2. The following vector field has zero traction derivative in x at the surface $x_3 = 0$:

$$v(x,y) = \left(-\frac{(2\,\mu + \lambda)\,(x_1 - y_1)^2}{\lambda}, 0, (x_1 - y_1)\,(x_3 - y_3) + (x_1 - y_1)\,(x_3 + y_3) \right).$$

In other words, calculations indicate that $T_{e_3(x)}v = (0,0,0)$ at $x_3 = 0$. Let A be the 3×3 matrix (v,v,v). A computation indicates that $T_{e_3(x)}A$ does not depend on y. Accordingly, $(T_{e_3(y)}T_{e_3(x)}A)^T$ is zero. The first column of $(T_{e_3(y)}A)^T$ is $(-2\mu x_3, -2\mu x_3, -2\mu x_3)$, and, thus, the first column of $T_{e_3(x)}(T_{e_3(y)}A)^T$ is $(-2\mu^2, -2\mu^2, -2\mu(2\mu+\lambda))$.

Example 3. We computed Mindlin's tensor, following a method that proceeds along the same lines as those sketched earlier in this present paper for the calculation of our Green's tensor H: we started from Kelvin's tensor G, which we reflected about the plane $x_3 = 0$, and finally three Boussinesq problems had to be solved. The case of Mindlin's tensor is computationally less intensive, as it involves terms of smaller degree than that of terms involved in the computation of Green's tensor H. Nevertheless, we found it worthwhile to utilize a symbolic computation software for two reasons: first, this certainly reduces chances of obtaining a wrong result; and, second, it makes it more convenient for verifying the final answer. Verification was made by validating elasticity equations, and decay at infinity, and order of growth near singularities and checking traction free boundary conditions.

In the end we found that although $T_{e_3(x)}M(x,y)$ is zero at $x_3 = 0$, $T_{e_3(x)}(T_{e_3(y)}M(x,y))^T$ is not zero at $x_3 = 0$, whereas previously $M(x,y)$ was Mindlin's tensor. The reason why this was not picked up in previous studies in natural sciences

may lie in the following observation: $M(x,y)$ is homogeneous in (x,y) of degree -1, and, consequently, $T_{e_3(x)}(T_{e_3(y)}M(x,y))^T$ is homogeneous in (x,y) of degree -3. If this tensor is evaluated for y_3 at some depth d beneath the surface $x_3 = 0$, the error in surface traction $T_{e_3(x)}(T_{e_3(y)}M(x,y))^T$ decays as d^{-3}, which is one order of magnitude smaller than displacements on the surface. In other words, using $T_{e_3(y)}M(x,y)$ for computing surface displacements due to a slip on a fault may lead to gross discrepancies, only if that fault is shallow and for those surface points close enough to the fault.

4. Application: Computations of displacement fields caused by a slip along a fault. In this section we use Green's tensor H introduced in this paper to compute displacement fields u due to a slip on a fault Γ, in the half space $x_3 < 0$, with traction free conditions on the surface $x_3 = 0$. In other words, u satisfies (15)–(18). This equation for u plays an important role in geophysics models. It may be used in the study of quasi-static displacements near a fault during a "silent earthquake" episode. Accounts of silent earthquakes in subduction zones near Japan [12] and New Zealand, Alaska, and Mexico [13, 11] were recently reported in the literature. This equation for u may also be used to study the nucleation phase (occurring after destabilization of faults and before the onset of seismic waves) for dynamically active faults. The earthquake nucleation phase, which precedes dynamic rupture, was uncovered by detailed seismological observations [14, 16] and identified in laboratory experiments [15, 17].

Typical length scales attached to faults observed in nature range from 0 to 100 kilometers for depth and 1 to 100 kilometers for length. During destabilization, slip on faults are on the order of 1 to 100 meters. Accordingly, in all numerical simulations in this section, we choose one kilometer to be the unit length for spatial coordinates, while surface displacements are given in meters. The Lamé coefficients are set to be $\lambda = \mu = 1$, a common choice in geophysics. This choice of λ and μ is not necessary for our computations to run faster or more accurately. It was rather made in order to facilitate comparisons to other pieces of work.

4.1. Exact field in two numerical examples. Recall that the displacement field u due to a slip g on a fault Γ, in the half space $x_3 < 0$, with traction free conditions on the surface $x_3 = 0$, that is, the solution to problem (15)–(18), can be expressed as $u = \frac{1}{2}\int_\Gamma Hg$. We compute in this section the displacement u on the surface $x_3 = 0$ using this integral formula in two examples.

These two examples involve the same fault geometry: Γ is contained in the plane normal to the vector $(1,0,1)$ and is bounded by an ellipse centered at $(0,0,-2)$. In local coordinates the ellipse has the equation $\tilde{y_1}^2 + (\tilde{y_2}/5)^2 = 1$, where local coordinates are related to the original coordinates by

$$y = \begin{pmatrix} s & 0 & s \\ 0 & 1 & 0 \\ -s & 0 & s \end{pmatrix} \tilde{y} + \begin{pmatrix} 0 \\ 0 \\ -2 \end{pmatrix}, \quad s = \frac{1}{\sqrt{2}}. \tag{44}$$

A sketch of this cross section appears in Figure 1.

In the first example slip occurs only in the e_2 direction. In local coordinates the slip was picked to be $g = C_1\sqrt{1 - \tilde{y_1}^2 - (\tilde{y_2}/5)^2}e_2$, where the constant C_1 was adjusted in such a way that the total slip $\int_\Gamma g$ be of norm 1; see Figure 2 for a plot of resulting surface displacements. We wish to emphasize that this choice of slip g is not arbitrary; it corresponds to the expected dominant profile of slip occurring

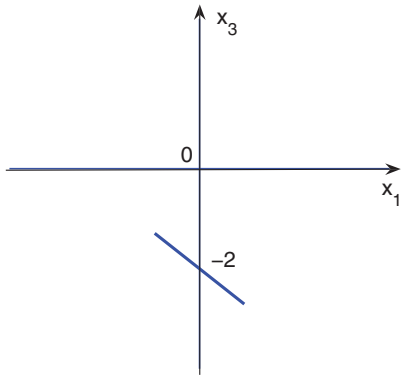

FIG. 1. *A cross section of the fault* Γ *involved in the first two numerical examples. The cross section is in the plane* $x_2 = 0$. *The small axis of the ellipse appears as the line segment in the cross section plane.*

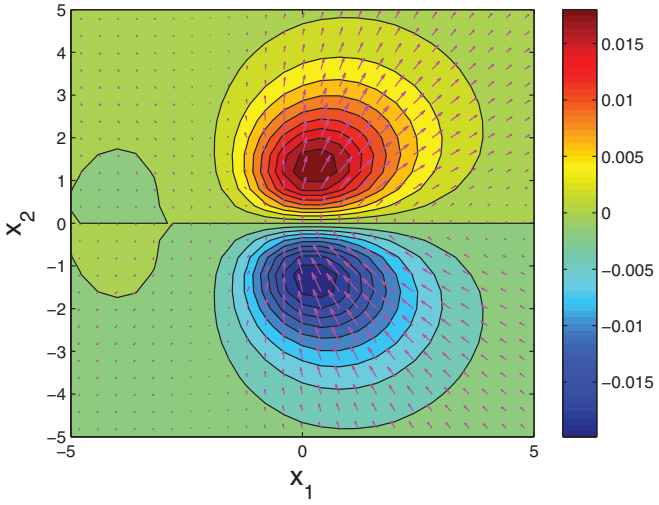

FIG. 2. *Computed surface displacement for the elliptic geometry and slip in the* e_2 *direction considered in the first example. In local coordinates the slip was picked to be* $g = C_1\sqrt{1-\tilde{y_1}^2-(\tilde{y_2}/5)^2}e_2$, *where the constant* C_1 *was adjusted in such a way that the total slip* $\int_\Gamma g$ *be of norm* 1. *The* e_1 *and* e_2 *components of* $u(x_1, x_2)$ *are represented as a planar vector field using arrows, while the* e_3 *component is sketched on the same graph using a color contour map.*

during the destabilization process of a fault. A complete theory for that process has been studied in the 2D case; see [2], [8], [9]. In the 3D case a complete theory is still being investigated, but analysis of relevant hypersingular operators suggests that slip occurring during the destabilization process of a fault decays toward the edge of the fault as the square root of the distance to this edge.

In the second example the slip does not have constant direction and is picked to be, in local coordinates, $g = C_2(-2m^{3/2}, m^{1/2}, 2m^{3/2})$, where $m = 1 - \tilde{y_1}^2 - (\tilde{y_2}/5)^2$ and the constant C_2 was adjusted, as previously, in such a way that the total slip $\int_\Gamma g$ still be of norm 1; see Figure 3 for a plot of resulting surface displacements.

4.2. Approximate field. Solving (15)–(18) by integrating $u = \frac{1}{2}\int_\Gamma Hg$ might be costly in number of operations, which is undesirable in applications where such a

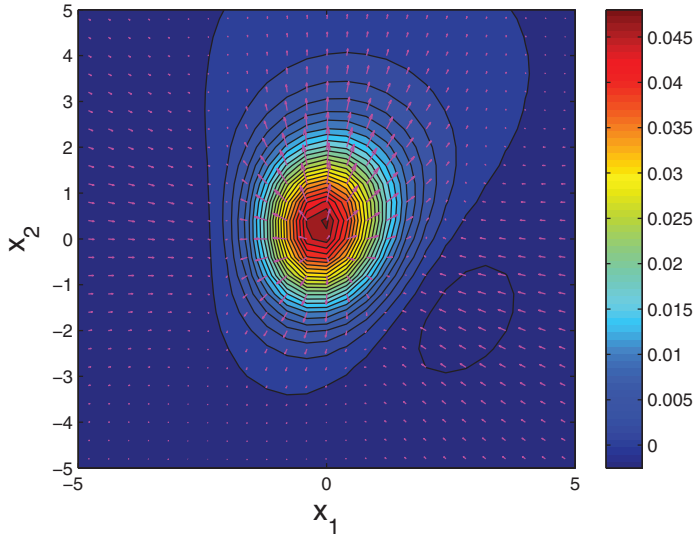

FIG. 3. *Computed surface displacements in the second example. The geometry of the fault is the same as in the first example; however, the slip does not in this case have constant direction and is picked to be, in local coordinates,* $g = C_2(-2m^{3/2}, m^{1/2}, 2m^{3/2})$, *where* $m = 1 - (\tilde{y_1}/5)^2 - \tilde{y_2}^2$ *and the constant* C_2 *was adjusted in such a way that the total slip* $\int_\Gamma g$ *be of norm* 1.

direct computation would have to be iterated a large number of times. We found a way to obtain a reasonable approximation to the field $u(x_1, x_2, 0)$ based on asymptotics that just assume that (x_1, x_2) is some distance away from the fault Γ. Suppose that the fault Γ is centered at the point (a, b, c) where $c < 0$. To obtain a simpler formula for the surface displacement $u(x_1, x_2, 0)$ we now assume that either the surface point (x_1, x_2) is far enough from (a, b) or $|c|$ is large enough. Thus, we may write

$$\begin{aligned} H(x_1, x_2, 0, y_1, y_2, y_3) &= H(x_1 - y_1, x_2 - y_2, 0, 0, 0, y_3) \\ &= H(x_1 - a, x_2 - b, 0, 0, 0, c) + O\left(\frac{1}{(x_1^2 + x_2^2 + c^2)^{3/2}}\right) \end{aligned}$$

as long as (y_1, y_2, y_3) remains on the fault Γ. From there, integrating over Γ,

$$u(x_1, x_2, 0) \simeq H(x_1 - a, x_2 - b, 0, 0, 0, c)\frac{1}{2}\int_\Gamma g(y_1, y_2, y_3)dy. \tag{45}$$

Setting $(t_1, t_2, t_3) = \frac{1}{2}\int_\Gamma g(y_1, y_2, y_3)dy$, we obtain

$$u(x_1, x_2, 0) \simeq H(x_1 - a, x_2 - b, 0, 0, 0, c)(t_1, t_2, t_3). \tag{46}$$

The vector $t := (t_1, t_2, t_3)$ can be interpreted as half the average slip on Γ times the area of Γ. We will call $2t$ the total slip on Γ.

We now proceed to demonstrate numerically the accuracy of approximation (46). We plot the relative L^2 error incurred in making the approximation (46) against depth for three different geometries in Figure 4. The L^2 error was computed on the surface $x_3 = 0$ in a square $[-10, 10] \times [-10, 10]$. In each case the fault was contained in the plane normal to the vector $(1, 0, 1)$ and passing through the center $(0, 0, c)$, where $|c|$ is the depth. Depth ranged from 2 to 20 in these numerical runs. Slip

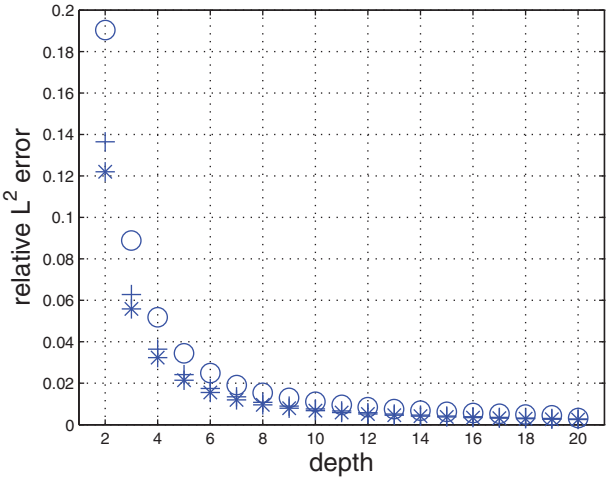

FIG. 4. *The relative L^2 error incurred by making the approximation* (46) *plotted against depth for the three different fault geometries discussed in section* 4.2.

was set to occur in the e_2 direction. Total slip was computed in order to apply formula (46). The plus markers correspond to a square geometry for Γ with edges of length 2. In local coordinates $(\tilde{y_1}, \tilde{y_2})$ centered on the fault, the slip was picked to be $\sqrt{(1-|\tilde{y_1}|)(1-|\tilde{y_2}|)}$. Local coordinates are now related to the original coordinates by

$$y = \begin{pmatrix} s & 0 & s \\ 0 & 1 & 0 \\ -s & 0 & s \end{pmatrix} \tilde{y} + \begin{pmatrix} 0 \\ 0 \\ c \end{pmatrix}, \quad s = \frac{1}{\sqrt{2}}.$$

The star markers correspond to Γ being a circle of radius 1. In local coordinates the slip was picked to be $\sqrt{1-\tilde{y_1}^2-\tilde{y_2}^2}$. The circular markers correspond to an elliptic geometry for Γ. The equation of the ellipse was picked to be, in local coordinates, $\tilde{y_1}^2 + (\tilde{y_2}/5)^2 = 1$. In local coordinates the slip was picked to be $\sqrt{1-\tilde{y_1}^2-(\tilde{y_2}/5)^2}$. The largest error is found for the most shallow faults, that is, for $|c| = 2$, and ranges from 12 to 19%, depending on geometry. We sketched the exact and approximated fields for faults at depth 2 in the elliptic geometry case in Figures 2 and 5. It appears that even at that shallow depth the exact and approximated profiles exhibit very similar patterns.

4.3. A symmetry property for deeper faults. Denote by $\tilde{u}$ the approximate surface displacement obtained by application of asymptotic formula (46). Accordingly, $\tilde{u} = Ht$. The coordinates of Ht are given in the appendix. Recall that symmetry property (35) corresponds to reversing the orientation on the fault Γ. A consequence of symmetry property (36) is that, for deeper faults, a total slip t on a planar fault Γ of normal vector n produces approximately the same surface displacements as in the "reversed case" of a total slip $n|t|$ on a planar fault Γ of normal vector $t/|t|$. Of course, this equivalence does not hold for shallow faults at surface points close to the fault.

Due to the expression for $H(x_1 - a, x_2 - b, 0, 0, 0, c)$ it turns out that $u(x_1, x_2)$ is

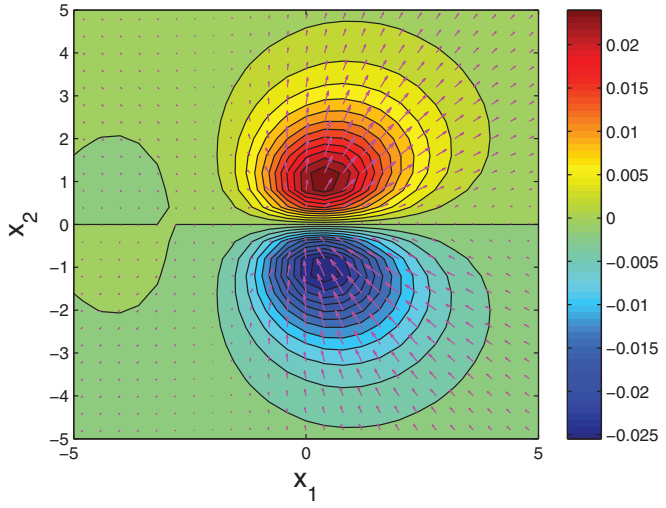

FIG. 5. *Approximate surface displacement for the elliptic geometry from Figure* 4 *at depth* 2. *The approximation was obtained by applying formula* (46). *The computed exact field is sketched in Figure* 2.

a function that depends on n and t only through s_0, s_1, s_2, s_3, and s_4 defined by

$$s_0 := n_1t_1 + n_2t_2, \tag{47}$$

$$s_1 := n_2t_3 + n_3t_2, \tag{48}$$

$$s_2 := n_1t_3 + n_3t_1, \tag{49}$$

$$s_3 := n_1t_2 + n_2t_1, \tag{50}$$

$$s_4 := n_1t_1 - n_2t_2. \tag{51}$$

Thus, one might wonder whether additional symmetries akin to (36) hold. The following proposition explains in detail how s_0, s_1, s_2, s_3, and s_4 relate to n and t if n and t are perpendicular. Note that, in the destabilization process of faults, previous studies have shown that the slip is tangential to the fault, so n and t are indeed perpendicular in that case.

PROPOSITION 4.1. *Assume that* $n = (n_1, n_2, n_3)$ *and* $t = (t_1, t_2, t_3)$ *are two orthogonal vectors in space such that* $|n| = 1$ *and* $|t| \neq 0$. *Given* s_0, s_1, s_2, s_3, *and* s_4 *defined by* (47)–(51) *exactly four different pairs* (n, t) *can be reconstructed. If* $(\tilde{n}, \tilde{t})$ *is one reconstructed pair, the other three are* $(-\tilde{n}, -\tilde{t})$, $(\frac{\tilde{t}}{|\tilde{t}|}, \tilde{n}|\tilde{t}|)$, *and* $(-\frac{\tilde{t}}{|\tilde{t}|}, -\tilde{n}|\tilde{t}|)$.

Proof. Form the matrix

$$D = \begin{pmatrix} 2n_1t_1 & s_3 & s_2 \\ s_3 & 2n_2t_2 & s_1 \\ s_2 & s_1 & 2n_3t_3 \end{pmatrix},$$

and notice that $D = nt^T + tn^T$. Denote $t' = t/|t|$ and $D' = D/|t| = nt'^T + t'n^T$. Since n and t' are orthogonal of norm 1, we have that $D't' = n$ and $D'n = t'$ from where it follows that $D'(n - t') = -(n - t')$ and $D'(n + t') = n + t'$. We conclude that $n - t'$ and $n + t'$ are eigenvectors for D for the respective eigenvalues $-|t|$ and $|t|$. Notice also that $n \times t$ is an eigenvector for the eigenvalue 0.

To reconstruct n and t, as D is real symmetric and has zero trace and determinant, we may denote by $-\alpha, 0, \alpha$ (with $\alpha > 0$) the eigenvalues of D.

To find a pair (n,t) from the symmetric matrix D we have to find two vectors v_1 and v_2 of norm $\sqrt{2}$ such that $Dv_1 = -\alpha v_1$ and $Dv_2 = \alpha v_2$. As D is symmetric v_1 and v_2 are orthogonal. If we then set $n = \frac{v_1 - v_2}{2}, t' = \frac{v_1 + v_2}{2}$, and $t = \alpha t'$, it is clear that the coordinates of (n,t) will satisfy (47)–(51) and so will the coordinates of the other pairs $(-n,-t), (\frac{t}{|t|}, n|t|)$, and $(-\frac{t}{|t|}, -n|t|)$.

Finally, we show that these are the only four solutions. This is because a basis for the eigenspace attached to the eigenvalue $-\alpha$ containing vectors of length $\sqrt{2}$ can only be given by either v_1 or $-v_1$, and a basis for the eigenspace attached to the eigenvalue α containing vectors of length $\sqrt{2}$ can only be given by either v_2 or $-v_2$; this gives a total number of four combinations. □

Remark. Assume that s_0, s_1, s_2, s_3, and s_4 are any five real numbers. Can we find two orthogonal vectors n and t such that $|n| = 1$ and (47)–(51) are satisfied? Forming the matrix

$$E = \begin{pmatrix} s_0 + s_4 & s_3 & s_2 \\ s_3 & s_0 - s_4 & s_1 \\ s_2 & s_1 & -2s_0 \end{pmatrix}$$

this is possible if and only if $\det(E) = 0$. Indeed, the condition $\det(E) = 0$ is necessary since $E(n \times t) = 0$. Conversely, as E is real and symmetric and its trace is zero, if $\det(E) = 0$, the eigenvalues of E must be $-\alpha, 0, \alpha$ for some $\alpha > 0$ unless $s_0 = s_1 = s_2 = s_3 = s_4 = 0$, in which case $E = 0$. The assertion then follows from the previous proposition.

To illustrate numerically the symmetry property, we computed the surface displacements $u(x_1, x_2)$ arising from the slip on the fault Γ of equation $\tilde{y_1}^2 + (\tilde{y_2}/5)^2 = 1$, in local coordinates, at depth $c = -2$ and normal to the vector $(\frac{1}{\sqrt{2}}, 0, \frac{1}{\sqrt{2}})$, where new and original coordinates are again related by (44). We imposed on that fault the slip $C_1(-2m^{3/2}, m^{1/2}, 2m^{3/2})$, where $m = 1 - \tilde{y_1}^2 - (\tilde{y_2}/5)^2$, in local coordinates, and the constant C_1 was computed such that the norm of the total slip $2t$ was 1. The computed profile appears in Figure 3.

Next, we proceeded to find the surface displacements for a reversed geometry, that is, the surface displacements $u'(x_1, x_2)$ arising from the slip on the fault Γ of equation $\tilde{y_1}^2 + (\tilde{y_2}/5)^2 = 1$, in local coordinates, at depth $c = -2$ and normal to the vector t with imposed slip $C_2((m/2)^{1/2} + 2m^{3/2})(1,0,1)$, where $m = 1 - \tilde{y_1}^2 - (\tilde{y_2}/5)^2$, in local coordinates, and the constant C_2 was computed such that the norm of the total slip was 1. The computed profile for $u'(x_1, x_2)$ appears in Figure 6.

We also computed the surface displacements $u''(x_1, x_2)$ obtained by application of asymptotic formula (46). The computed profile for $u''(x_1, x_2)$ appears in Figure 7.

Finally, we compared relative differences in the L^2 norm for u, u', and u'' where the surface domain of integration is $[-10, 10] \times [-10, 10]$. For example, the relative difference of u to u' is $\sqrt{\int |u - u'|^2 / \int |u|^2}$, where all integrals are over $[-10, 10] \times [-10, 10]$. We computed these relative differences for two depths $c = -2$ and $c = -20$, and we placed them in Table 1.

5. Conclusion. We have computed in this paper a double layer Green's tensor for linear elasticity in half space, with traction free conditions on the surface. Our approach starts from Kelvin's free space tensor: we first took a traction derivative, and then we made a long calculation whose goal was to derive additional terms accounting for the traction free boundary condition. We indicated the form of the final solution in the appendix. In effect, we are able to provide relatively concise formulas for H

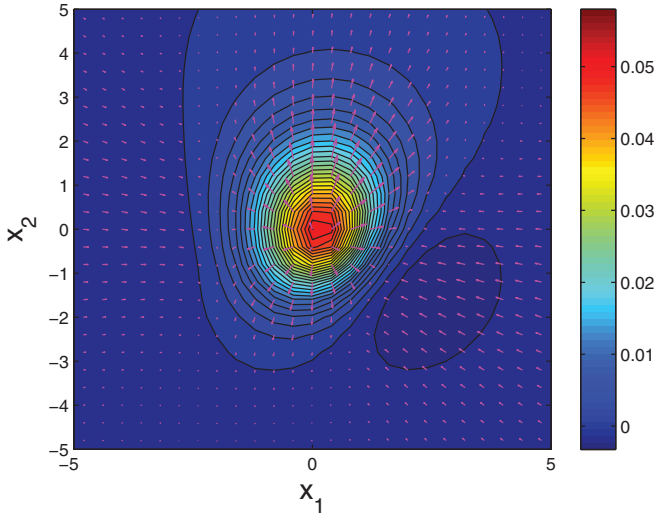

FIG. 6. *Surface displacements* $u'(x_1, x_2)$ *arising from the slip on the fault* Γ *of equation* $\tilde{y_1}^2 + (\tilde{y_2}/5)^2 = 1$*, in local coordinates, at depth* $c = -2$ *and normal to the vector* t *with imposed slip* $C_2((m/2)^{1/2} + 2m^{3/2})(1, 0, 1)$*, where* $m = 1 - (\tilde{y_1}/5)^2 - \tilde{y_2}^2$*, in local coordinates, and the constant* C_2 *is a computed constant ensuring that the norm of the total slip be* 1*. We observe that the displacement pattern is similar to the one plotted in Figure* 3.

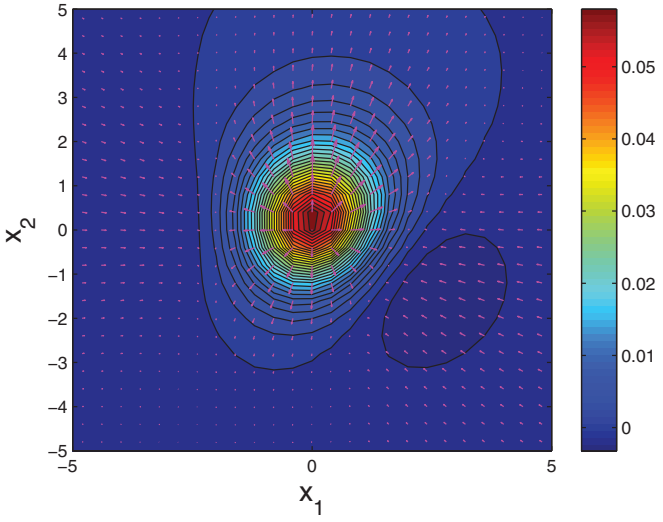

FIG. 7. *Surface displacements* $u''(x_1, x_2)$ *obtained by application of asymptotic formula* (46) *to either the case relative to Figure* 3 *or to the case relative to Figure* 6.

only on the surface $x_3 = 0$. For $x_3 < 0$, the simplest form for H is too lengthy, but still manageable on a computer system.

We also showed that simply starting from Mindlin's half space tensor and then taking a traction derivative leads to an incorrect result: the traction free condition on the surface is lost. This is due to the fact that traction operators do not commute. We illustrated this lack of commutativity on simple examples.

We demonstrated how our Green's tensor relates to 2D linear elasticity in a half

TABLE 1

Relative differences in the L^2 norm for u, u', and u'' where the domain of integration is $[-10,10]\times[-10,10]$. For example, the relative difference of u to u' is $\sqrt{\int |u-u'|^2 / \int |u|^2}$, where all integrals are over $[-10,10]\times[-10,10]$. We computed these relative differences for two depths $c=-2$ and $c=-20$.

	u to u'	u to u''	u' to u''
$c=-2$	.1814	.1741	.1738
$c=-20$	.002265	.002103	.001984

plane. That case reduces to recovering Green's scalar function in the lower half plane with zero Neumann condition on the surface. We also explained why under some decay and growth condition our Green's tensor is unique, and we use this uniqueness result to verify our calculation for H. Finally, we used our tensor H for the explicit numerical computation of surface displacement fields due to a slip on a crack, or fault, beneath the surface. As the exact solution might require an intensive computation, we found a way to obtain an approximate field $u(x_1, x_2, 0)$ based on asymptotics assuming only that (x_1, x_2) is some distance away from the fault Γ. This led to a discussion on an interesting symmetry property, valid for deeper faults.

The half space setting considered in this paper plays an important role in geophysics, where the traction free plane at the boundary models the surface of the Earth. This geometry may also be helpful in material science at adequate length scales. We have shown in this paper the expression in closed form for H on the surface and its use for efficiently approximating surface fields due to a slip on the fault. In another paper we will demonstrate how one can take advantage of those approximate closed form expressions for surface displacements, in order to solve the fault inverse problem: given a surface displacement field u, can one recover the fault and the slip that gave rise to u? We provide a positive answer to a regularized version of that problem. Our recovery method combines algebraic manipulations on the approximate closed form expressions for surface displacements to minimization techniques; see [10].

6. Appendix. Instead of giving formulas for each entry of the matrix H, it is advantageous to write out formulas for the coordinates $H\,t$, where t is the vector (t_1, t_2, t_3). We only present in this appendix formulas at $x_3 = 0$; the idea is to give a feel for the different terms involved. The complete formula for $x_3 < 0$ is best left within a computer code.

It proves convenient to introduce polar surface coordinates.

6.1. If $(x_1 - y_1)^2 + (x_2 - y_2)^2 = 0$. The three coordinates of $H\,t$ are then, respectively,

$$0,$$

$$0,$$

$$\frac{-\mu(n_1 t_1 + n_2 t_2) + 6(\lambda+\mu) n_3 t_3}{4\pi {y_3}^2\,(\lambda+\mu)}.$$

6.2. If $(x_1 - y_1)^2 + (x_2 - y_2)^2 > 0$. We set

$$\rho = \sqrt{(x_1 - y_1)^2 + (x_2 - y_2)^2},$$
$$d = \sqrt{\rho^2 + y_3^2},$$

$$c = \frac{x_1 - y_1}{\rho},$$
$$s = \frac{x_2 - y_2}{\rho}.$$

The first coordinate of $H\,t$ is the ratio of

$$\alpha n_1 t_1 + \beta n_2 t_2 + \gamma n_3 t_3 + \delta(n_1 t_2 + n_2 t_1) + \epsilon(n_1 t_3 + n_3 t_1) + \zeta(n_2 t_3 + n_3 t_2) \tag{52}$$

to

$$(\lambda + \mu)\pi\,\rho^3 d^5, \tag{53}$$

where, setting

$$A = \left(y_3 d\rho^4 + \left(\frac{5}{2}\,{y_3}^4 + 2\,{y_3}^3 d\right)\rho^2 + {y_3}^6 + {y_3}^5 d\right)\mu\,,$$

$\alpha, \beta, \gamma, \delta, \gamma, \epsilon$, and ζ are given by

$$\frac{\alpha}{c} = -A\left(4\,c^2 - 3\right) + \left(\frac{3}{2}\,\lambda\,c^2 + \mu\right)\rho^6 - \frac{1}{2}\,\mu\,\left(15\,c^2 - 11\right){y_3}^2\rho^4,$$
$$\frac{\beta}{c} = A\left(4\,c^2 - 3\right) - \frac{3}{2}\,\lambda\,\left(c^2 - 1\right)\rho^6 + \frac{3}{2}\,\mu\,\left(5\,c^2 - 4\right){y_3}^2\rho^4,$$
$$\frac{\gamma}{c} = \frac{3}{2}\,(\lambda + \mu){y_3}^2\rho^4,$$
$$\frac{\delta}{s} = -A\left(4\,c^2 - 1\right) + \left(\frac{3}{2}\,\lambda\,c^2 + \frac{1}{2}\,\mu\right)\rho^6 - \frac{1}{2}\,\mu\,\left(15\,c^2 - 4\right){y_3}^2\rho^4,$$
$$\epsilon = -\frac{3}{2}\,\rho^5 y_3 c^2(\lambda + \mu),$$
$$\zeta = -\frac{3}{2}\,(\lambda + \mu)cs y_3\rho^5.$$

The second coordinate of $H\,t$ is also in the form of a ratio of (52) to (53), where this time $\alpha, \beta, \gamma, \delta, \gamma, \epsilon$, and ζ are given by

$$\frac{\alpha}{s} = -A\left(4\,c^2 - 1\right) + \frac{3}{2}\,\lambda\,c^2\rho^6 - \frac{3}{2}\,\left(5\,c^2 - 1\right)\mu\,{y_3}^2\rho^4,$$
$$\frac{\beta}{s} = A\left(4\,c^2 - 1\right) + \left(\frac{3}{2}\,\lambda + \mu - \frac{3}{2}\,\lambda\,c^2\right)\rho^6 + \frac{1}{2}\,\mu\,\left(-4 + 15\,c^2\right){y_3}^2\rho^4,$$
$$\frac{\gamma}{s} = \frac{3}{2}\,(\lambda + \mu){y_3}^2\rho^4,$$
$$\frac{\delta}{c} = A\left(4\,c^2 - 3\right) + \left(\frac{3}{2}\,\lambda + \frac{1}{2}\,\mu - \frac{3}{2}\,\lambda\,c^2\right)\rho^6 + \frac{1}{2}\,\mu\,\left(15\,c^2 - 11\right){y_3}^2\rho^4,$$
$$\epsilon = -\frac{3}{2}\,(\lambda + \mu)cs y_3\rho^5,$$
$$\zeta = \frac{3}{2}\,\rho^5 y_3\left(c^2 - 1\right)(\lambda + \mu).$$

Setting

$$B = \left(\frac{1}{2}\, d\rho^5 + d{y_3}^2\rho^3 + \left(\frac{1}{2}\, {y_3}^5 + \frac{1}{2}\, {y_3}^4 d\right)\rho\right)\mu\,,$$

the third coordinate of $H\,t$ is also in the form of a ratio of (52) to (53), where this time $\alpha, \beta, \gamma, \delta, \gamma, \epsilon$, and ζ are given by

$$\alpha = -B\left(-1 + 2\,c^2\right) + \left(-3\,\mu\,c^2 - \frac{3}{2}\,\lambda\,c^2 + \mu\right) y_3\rho^5 - \frac{1}{2}\,\mu\,\left(5\,c^2 - 3\right) {y_3}^3\rho^3,$$

$$\beta = B\left(-1 + 2\,c^2\right) + \left(-2\,\mu + \frac{3}{2}\,\lambda\,c^2 - \frac{3}{2}\,\lambda + 3\,\mu\,c^2\right) y_3\rho^5 + \frac{1}{2}\,\mu\,\left(-2 + 5\,c^2\right) {y_3}^3\rho^3,$$

$$\gamma = -\frac{3}{2}\,(\lambda + \mu){y_3}^3\rho^3,$$

$$\frac{\delta}{sc} = \left(\left(-\frac{3}{2}\,\lambda - 3\,\mu\right) y_3 - d\mu\right)\rho^5 + \left(-\frac{5}{2}\,\mu\,{y_3}^3 - 2\,d\mu\,{y_3}^2\right)\rho^3 + \left(-d\mu\,{y_3}^4 - \mu\,{y_3}^5\right)\rho,$$

$$\frac{\epsilon}{c} = \frac{3}{2}\,(\lambda + \mu){y_3}^2\rho^4,$$

$$\frac{\zeta}{s} = \frac{3}{2}\,(\lambda + \mu){y_3}^2\rho^4.$$

Remark. Denote by (u_1, u_2, u_3) the coordinates of Ht, whose expressions were given above. From (33) and (34) the following symmetry properties must hold:

$$u_1(s, c, n_1, n_2, t_1, t_2) = u_2(c, s, n_2, n_1, t_2, t_1),$$
$$u_3(s, c, n_1, n_2, t_1, t_2) = u_3(c, s, n_2, n_1, t_2, t_1).$$

These symmetry properties can be directly verified from the previous formulas using that $s^2 + c^2 = 1$.

Acknowledgments. The author wishes to thank Prof. I. R. Ionescu for his offering of important suggestions and helpful comments.

REFERENCES

[1] M. Abramowitz and I. Stegun, eds., *Handbook of Mathematical Functions with Formulas, Graphs, and Mathematical Tables,* Dover, New York, 1992.

[2] C. Dascalu and I. R. Ionescu, *Slip weakening friction instabilities: Eigenvalue analysis,* Math. Models Methods Appl. Sci., 14 (2004), pp. 439–459.

[3] P. A. Martin, L. Päivärinta, and S. Rempel, *A normal crack in an elastic half-space with stress-free surface. English summary,* Math. Methods Appl. Sci., 16 (1993), pp. 563–579.

[4] R. D. Mindlin, *Force at a point in the interior of a semi infinite solid,* Phys., 7 (1936), pp. 195–202.

[5] V. Z. Parton and P. I. Perlin, *Integral Equations in Elasticity,* Mir, Moscow, 1982. MR 509209 (80a:73001)

[6] J. A. Steketee, *On Volterra's dislocations in a semi infinite elastic medium,* Canad. J. Phys., 36 (1958), pp. 192–205.

[7] G. Y. Sheu, *Deformations caused by the movements of shear and tensile faults,* Int. J. Numer. Anal. Methods Geomech., 25 (2001), pp. 1175–1193.

[8] I. R. Ionescu and D. Volkov, *An inverse problem for the recovery of active faults from surface observations,* Inverse Problems, 22 (2006), pp. 2103–2121.

[9] I. R. Ionescu and D. Volkov, *Earth surface effects on active faults: An eigenvalue asymptotic analysis*, J. Comput. Appl. Math., 220 (2008), pp. 143–162.

[10] I. R. Ionescu and D. Volkov, *Detecting tangential dislocations on planar faults from traction free surface observations*, Inverse Problems, 25 (2009), 015012.

[11] V. Kostoglodov, S. K. Singh, J. A. Santiago, S. I. Franco, K. M. Larson, A. R. Lowry, and R. Bilham, *A large silent earthquake in the Guerrero seismic gap, Mexico,* Geophys. Res. Lett., 30 (2003) citation 1807.

[12] T. Sagiya and S. Ozawa, *Anomalous transient and silent earthquakes along the Nankai Trough subduction zones,* Seismol. Res. Lett., 73 (2002), pp. 234–235.

[13] A. R. Lowry, K. M. Larson, V. Kostoglodov, and O. Sanchez, *The fault slip budget in Guerrero, Southern Mexico,* Geophys. J. Int., 200 (2005), pp. 1–15.

[14] Y. Iio, *Slow initial phase of the P-wave velocity pulse generated by microearthquakes,* Geophys. Res. Lett., 19 (1992), pp. 477–480.

[15] J. H. Dieterich, *A model for the nucleation of earthquake slip*, in Earthquake Source Mechanics, Geophys. Monogr. Ser. 37, S. Das, J. Boatwright, and C.H. Scholz, eds., American Geophysical Union, Washington, D. C., 1986, pp. 37–47.

[16] W. L. Elsworth and G. C. Beroza, *Seismic evidence for an earthquake nucleation phase,* Sci., 268 (1995), pp. 851–855.

[17] M. Ohnaka, Y. Kuwakara, and K. Yamamoto, *Constitutive relations between dynamic physical parameters near a tip of the propagation slip during stick-slip shear failure,* Tectonophysics, 144 (1987), pp. 109–125.